

Optimization of Edge Directions and Weights for Mixed Guidance Graphs in Lifelong Multi-Agent Path Finding

Yulun Zhang¹, Varun Bhatt², Matthew C. Fontaine^{3*}, Stefanos Nikolaidis² and Jiaoyang Li¹

¹Robotics Institute, Carnegie Mellon University ³Lila Sciences

²Thomas Lord Department of Computer Science, University of Southern California

yulunzhang@cmu.edu, vsbhatt@usc.edu, mfontaine@lila.ai, nikolaid@usc.edu, jiaoyangli@cmu.edu

Abstract

Multi-Agent Path Finding (MAPF) aims to move agents from their start to goal vertices on a graph. Lifelong MAPF (LMAPF) continuously assigns new goals to agents as they complete current ones. To guide agents' movement in LMAPF, prior works have proposed Guidance Graph Optimization (GGO) methods to optimize a guidance graph, which is a bidirected weighted graph whose directed edges represent moving and waiting actions with edge weights being action costs. Higher edge weights represent higher action costs. However, edge weights only provide *soft* guidance. An edge with a high weight only *discourages* agents from using it, instead of *prohibiting* agents from traversing it. In this paper, we explore the need to incorporate edge directions optimization into GGO, providing *strict* guidance. We generalize GGO to Mixed Guidance Graph Optimization (MGGO), presenting two MGGO methods capable of optimizing both edge weights and directions. The first optimizes edge directions and edge weights in two phases separately. The second applies Quality Diversity algorithms to optimize a neural network capable of generating edge directions and weights. We also incorporate traffic patterns relevant to edge directions into a GGO method, making it capable of generating edge-direction-aware guidance graphs.

1 Introduction

We study the problem of leveraging a mixed guidance graph with optimized edge weights and directions to guide agents' movement, improving throughput of LMAPF algorithms. Multi-Agent Path Finding (MAPF) [Stern *et al.*, 2019] aims to move agents from their corresponding start to goal vertices on a given graph G without collisions, while lifelong MAPF (LMAPF) [Li *et al.*, 2021] continuously assigns new goal vertices to agents while they finish the current ones. Applications of LMAPF include autonomous warehouses [Li *et al.*, 2021], robotic sorting systems [Zhang *et al.*, 2025], and video games [Ma *et al.*, 2017; Jansen and Sturtevant, 2008].

*Work done before joining Lila Sciences.

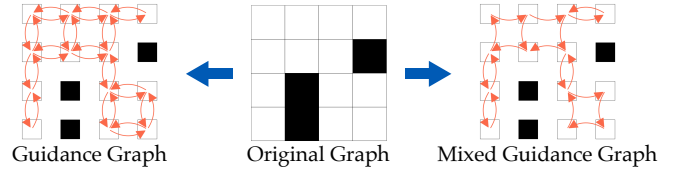


Figure 1: A guidance graph and a mixed guidance graph defined for a grid graph. Edge weights are all 1 for simplicity.

LMAPF problems are solved by decomposing them into a sequence of MAPF instances and solving them in order. Inevitably, planned paths are myopic, which could result in traffic congestion. To mitigate this issue, Zhang *et al.* [2024] propose a guidance graph, a bidirected weighted graph in which each directed edge (u, v) represents a moving or waiting action from vertex u to v and its weight represents the action cost, where higher weights represent higher costs. Agents are asked to plan paths that minimize the sum of action costs on the guidance graph. Two Guidance Graph Optimization (GGO) techniques are presented to optimize the edge weights with the objective of maximizing throughput, defined as the number of goals reached per timestep. A well-optimized guidance graph reduces traffic congestion by encouraging agents to move in the same direction on an edge.

However, for a high-weight edge, agents can use it if it results in a smaller overall cost, resulting in head-on collisions, which happens when agents travel in opposite directions on the same edge. Resolving a head-on collision in MAPF is challenging, as it requires at least one of the agents to take a detour. This issue can be amplified if agents move in more realistic motion models. For example, if agents move under the rotation motion model [Jiang *et al.*, 2024], in which agents can only move forward and rotate in place, taking a detour can take longer than with the pebble motion model [Stern *et al.*, 2019], where agents move omni-directionally, because of the additional rotation actions. Since the rotational model more accurately reflects the motion of differentiable drives commonly used in real-world LMAPF applications, including autonomous warehouses [Yan and Li, 2025] and robotic sorting systems [Kou *et al.*, 2020], it is desirable to optimize edge directions, determining which edges to block.

Optimizing edge directions is a non-trivial problem. First, we need to guarantee strong connectivity. All pairs of ver-

tices of the graph must be reachable from each other. Second, blocking too many edges might force agents to take unnecessary detours. We need a technique that considers the trade-off between reducing head-on collisions and shortening agents’ travel distances. Therefore, in this paper, we explore whether the incorporation of edge direction optimization into GGO can help improve throughput. We generalize GGO to Mixed Guidance Graph Optimization (MGGO), which optimizes both edge weights and directions, and present two MGGO methods. Figure 1 shows an example of a mixed guidance graph compared to a guidance graph. To ensure strong connectivity, we introduce a simple algorithm to repair the graph. In addition, we incorporate edge-direction-related information into the optimization process of a GGO method, making it optimize *edge-direction-aware* guidance graphs.

We make the following contributions: (1) generalizing the guidance graph to the mixed guidance graph as a more general representation of the guidance for LMAPF, (2) proposing two MGGO methods, showing their superior performance compared to state-of-the-art GGO methods, and (3) providing insights into the trade-off of edge weights and edge directions as different means of representing guidance for LMAPF.

2 Background

2.1 Lifelong Multi-Agent Path Finding

Since the rotational motion model [Jiang *et al.*, 2024] can model robots of real-world applications of LMAPF more realistically than the pebble motion model [Stern *et al.*, 2019], this paper focuses primarily on the MAPF and LMAPF problems defined on the rotational motion model.

Definition 1 (MAPF). *Given a four-connected 2D grid graph $G(V, E)$ and k agents with their start and goal vertices in G , MAPF aims to find collision-free paths from the start to the goal vertices. The state of each agent is determined by its current vertex $v \in V$ and its orientation $o \in \{\text{North, South, East, West}\}$. In each discretized timestep, agents can move forward to an adjacent vertex, rotate 90° , or wait. Two agents collide if they arrive at the same vertex or move through the same edge from opposite directions at the same timestep. MAPF minimizes the sum-of-cost, the sum of path length of all agents.*

Definition 2 (LMAPF). *Lifelong MAPF (LMAPF) is a variant of MAPF in which agents are continuously assigned new goal vertices when they arrive at the current ones. LMAPF maximizes throughput, the average number of goal vertices reached by all agents at each timestep.*

To solve LMAPF, Silver [2005] proposes WHCA*, which uses priority planning [Erdmann and Lozano-Perez, 1986] to find collision-free paths for all agents within a pre-defined planning window. RHCR [Li *et al.*, 2021] advances this idea to using any MAPF algorithm to search for collision-free paths within a planning window w every h timesteps ($w \geq h$). Instead of explicitly searching for collision-free paths, rule-based algorithms Wang and Botea [2008] move agents step by step by following a set of pre-defined rules. PIBT [Okumura *et al.*, 2019] is a ground-breaking work in

this category that moves by selecting their most preferred actions in each step. If collisions occur, a pre-defined rule based on priority inheritance and backtracking is applied to resolve the collisions. Yuhnevich and Andreychuk [2025] extends PIBT by planning multiple steps. To show that our proposed MGGO methods work for different types of LMAPF algorithms, we select RHCR [Li *et al.*, 2021] and PIBT [Okumura *et al.*, 2019; Jiang *et al.*, 2024] to conduct the experiments.

2.2 Edge Weights as Guidance

Many prior works have represented guidance as edge weights in MAPF. However, they mostly manually design or use handcrafted equations to generate the edge weights. Cohen *et al.* [2015] proposes the concept of highways, which selects a set of preferred edges as highways and assigns a lower edge weight to them, encouraging agents to traverse the highways. Cohen *et al.* [2016] generates highways based on handcrafted equations, but does not outperform Crisscross [Cohen, 2020; Li and Sun, 2023], which manually designs highways by alternating directions in even and odd rows and columns. Meanwhile, Jansen and Sturtevant [2008] assigns a direction vector to every vertex in G , and computes a movement cost based on past traffic using a handcrafted equation. More recent works apply a similar idea to collect traffic patterns and use handcrafted equations to compute edge weights [Han and Yu, 2022; Yu and Wolf, 2023; Chen *et al.*, 2024]. Attempting to unify the prior works, Zhang *et al.* [2024] propose the guidance graph.

Notation. For a pair of vertices u and v , we use $\{u, v\}$ and (u, v) to denote undirected and directed edges, respectively. The connection between u and v is bidirected if both (u, v) and (v, u) exist. The connection is unidirectional if exactly one of (u, v) and (v, u) exists.

Definition 3 (Guidance Graph). *Given a connected graph $G(V, E)$ for LMAPF, a guidance graph $G_g(V, E_g, \omega)$ is a bidirected weighted graph where each directed edge $(u, v) \in E_g$, $u, v \in V$, corresponds to an action that agents can take in G to move from u to v . $E_g = E_{wr} \cup E_{move}$, where E_{wr} contains self-loops where $u = v$, representing waiting or rotating. E_{move} contains edges with $u \neq v$, representing moving forward. All edge weights are represented as a vector $\omega \in \mathbb{R}_{>0}^{|E_g|}$.*

Definition 4 (Guidance Graph Optimization). *Given a graph $G(V, E)$, an objective function $f : \mathbb{R}^{|E_g|} \rightarrow \mathbb{R}$, and lower and upper bounds ω_{lb} and ω_{ub} ($0 < \omega_{lb} \leq \omega_{ub}$) for edge weights, GGO searches for the best guidance graph $G_g^*(V_g, E_g, \omega^*)$ with*

$$\omega^* = \arg \max_{\omega_{lb} \leq \omega \leq \omega_{ub}} f(\omega) \quad (1)$$

Zhang *et al.* [2024] propose two GGO methods. They first propose GGO Direct Search (GGO-DS), which uses the Covariance Matrix Adaptation Evolutionary Strategy (CMA-ES) [Hansen, 2016], a black-box optimizer, to directly search for all edge weights with the objective of maximizing throughput. CMA-ES maintains a multi-variate Gaussian distribution to model the edge weights. Starting from a standard normal Gaussian, GGO-DS iteratively samples new

batches of edge weights from the Gaussian. To ensure that the edge weights satisfies the pre-defined range, GGO-DS uses min-max normalization. After evaluation, the mean and covariance matrix of the Gaussian is updated to the high-throughput region of the search space. However, CMA-ES scales poorly as the number of edges in the guidance graph increases. Therefore, they propose GGO Parameterized Iterative Update (GGO-PIU), which uses a neural-network-based *update model* to generate edge weights in an iterative manner. Starting from an unweighted guidance graph where all edge weights are 1, PIU runs LMAPF simulations to collect the frequency of waiting at each vertex and uses the update model to update edge weights. PIU runs for N_p iterations. The model is optimized by CMA-ES to maximize throughput.

GGO-PIU has several weaknesses. First, it requires running at least one LMAPF simulation in each iteration, which is computationally expensive. For example, PIU does not work for RHCR [Zhang *et al.*, 2024]. Second, the edge weights of the initial guidance graph are 1. Intuitively, a better initial guidance graph can provide more hints to the update model, making it easier for the model to generate better guidance graphs. To tackle these weaknesses, we propose to use Parameterized Update (PU), a variant of PIU with $N_p = 1$.

2.3 Edge Directions as Guidance

Although many works have studied edge weights as guidance, similar studies on edge directions are relatively limited. In MAPF, no prior works have studied edge directions optimization. The directed Crisscross pattern [Wang and Botea, 2008; Li and Sun, 2023] is a common manually designed pattern of edge directions. It is a variant of Crisscross, in which only the preferred edges are kept in the graph. However, directed Crisscross can only be generated from biconnected graphs, which are undirected graphs that do not have bridges. A bridge is an undirected edge in an undirected graph whose removal disconnects the graph.

In urban traffic network design and navigation of multiple Automated Guided Vehicles, a similar problem of Strong Network Orientation Problem (SNOP) [Duhamel and Santos, 2024] is studied. Given an undirected graph, SNOP determines a direction for each undirected edge in the graph so that the resulting directed graph is strongly connected and the total distance between each pair of vertices is optimized. Robbins [1939] has established that directions can be assigned to the edges of a biconnected graph to make it strongly connected. As an NP-hard problem [Burkard *et al.*, 1999], existing works solve SNOP by using Mixed Integer Linear Programming (MILP) [Gaskins and Tanchoco, 1987; Duhamel and Santos, 2024], Branch-and-Bound [Kaspi and Tanchoco, 1990], and neighborhood search [Gallo *et al.*, 2010]. However, it is non-trivial to adapt these methods to optimize edge directions for MAPF. First, they do not scale to large graphs with thousands of vertices. Second, they do not optimize throughput. Third, they enforce strong connectivity using MILP [Duhamel and Santos, 2024], which scales poorly, or naive rejection sampling [Gallo *et al.*, 2010], which is not sample efficient.

2.4 Quality Diversity Algorithm

QD algorithms optimize an objective and diversify a set of diversity measures simultaneously. A measure space is defined based on the given diversity measures and it is evenly discretized into cells, referred to as an *archive*. QD attempts to find the best solution in each cell, optimizing the QD-score, defined as the sum of objective values of all solutions in the archive. Covariance Matrix Adaptation MAP-Annealing (CMA-MAE) [Fontaine and Nikolaidis, 2023] is the state-of-the-art QD algorithm for continuous search spaces. Similar to CMA-ES, it maintains, samples, and updates a multi-variate Gaussian distribution to optimize QD-score. Although QD methods are used primarily to generate diverse high-quality solutions [Fontaine *et al.*, 2021; Bhatt *et al.*, 2022], prior work has shown both theoretically [Qian *et al.*, 2024] and empirically [Zhang *et al.*, 2023] that diversity measures can assist objective optimization.

3 Problem Definition

Definition 5 (Mixed Guidance Graph). *Given a connected undirected graph $G(V, E)$, a mixed guidance graph $G_{mg}(V, E_{mg}, \omega_{mg})$ is a directed weighted graph. For each non-bridge undirected edge $\{u, v\} \in E$, we add (u, v) or (v, u) or both (u, v) and (v, u) to E_{mg} . For each bridge $\{u, v\}$, we add both (u, v) and (v, u) to E_{mg} . $\forall v \in V$, we also add (v, v) to E_{mg} . All edge weights are represented as a vector $\omega_{mg} \in \mathbb{R}_{>0}^{|E_{mg}|}$.*

To plan with a mixed guidance graph without compromising feasibility, we change the objective of MAPF from sum-of-costs to sum of action costs on the mixed guidance graph G_{mg} , similar to Zhang *et al.* [2024].

Definition 6 (Mixed Guidance Graph Optimization). *Given a connected unweighted graph $G(V, E)$, an objective function $f : \mathcal{G}_{mg} \rightarrow \mathbb{R}$, where \mathcal{G}_{mg} is the space of all mixed guidance graphs, and lower and upper bounds ω_{lb} and ω_{ub} ($0 < \omega_{lb} \leq \omega_{ub}$) for edge weights, the Mixed Guidance Graph Optimization (MGGO) problem searches for the optimal mixed guidance graph $G_{mg}^*(V, E_{mg}^*, \omega_{mg}^*)$ with:*

$$G_{mg}^* = \arg \max_{G_{mg} \in \mathcal{G}_{mg}} f(G_{mg}) \quad (2)$$

$$s.t. \quad G_{mg} \text{ is strongly connected} \quad (3)$$

$$\omega_{lb} \leq \omega_{mg} \leq \omega_{ub} \quad (4)$$

4 Approach

We first introduce a simple algorithm to repair a given graph for strong connectivity. We then present three approaches to incorporate edge directions. The first two are MGGO methods: one searches for a mixed guidance graph by optimizing edge weights and directions in two separate phases, and the other optimizes both simultaneously. The third approach only optimizes edge weights via GGO-PU, but is guided by information from manually designed mixed guidance graphs with unidirectional edges.

Algorithm 1: Edge Reversal Search (ERS)

Input: $G_{in} = (V_{in}, E_{in})$: a mixed guidance graph.
 E_b : bridge edges.
`tarjanAlgo`: Function that runs Tarjan algorithm and return the SCCs and the number of SCCs.
`buildCondenseGraph`: Function to build a condensation graph on the SCCs of G_{in} .
`outgoingEdges`: Function to find the outgoing edges of vertices in G_{in} in the SCC corresponding to a meta vertex.
`ReverseEdge`: Function to reverse the edge direction.
Output: A strongly connected mixed graph obtained by reversing edge directions.

```
1 if  $E_b \not\subseteq E_{in}$  then
2    $E_{in} \leftarrow E_{in} \cup \bigcup_{\{u,v\} \in E_b} \{(u,v), (v,u)\}$ ;
3  $scc, C \leftarrow \text{tarjanAlgo}(G_{in})$ ;
4 while  $C > 1$  do
5    $\mathcal{D}(\mathcal{V}, \mathcal{E}) \leftarrow \text{buildCondenseGraph}(G_{in}, scc, C)$ ;
6    $\eta \leftarrow$  a meta vertex s.t.  $\eta \in \mathcal{V}$  &  $\text{deg}^-(\eta) = 0$ ;
7    $E_{out} \leftarrow \text{outgoingEdges}(G_{in}, \eta)$ ;
8    $E_{rev} \leftarrow \text{sample} \lfloor \frac{|E_{out}|}{2} \rfloor$  distinct edges from  $E_{out}$ ;
9   for  $(u,v) \in E_{rev}$  do
10     $\text{ReverseEdge}(G_{in}, (u,v))$ ;
11   $scc, C \leftarrow \text{tarjanAlgo}(G_{in})$ ;
12 return  $G_{in}$ ;
```

4.1 Edge Reversal Search

We propose **Edge Reversal Search (ERS)**, a greedy algorithm to repair a given mixed guidance graph for strong connectivity by reversing edge directions. Algorithm 1 shows the pseudocode. Given an input mixed graph $G_{in}(V_{in}, E_{in})$ and all bridges E_b in the original undirected graph G corresponding to G_{in} , we first add (u,v) and (v,u) for all bridges $\{u,v\} \in E_b$ to E_{in} (algorithm 1) because these edges must be present to ensure strong connectivity. Bridges can be easily found in G by using a linear-time algorithm based on DFS [Tarjan, 1974]. We then run Tarjan algorithm [Tarjan, 1972] to find all strongly connected components (SCC) of G_{in} (algorithm 1) and C , the number of SCCs. If there is more than 1 SCC (algorithm 1), then G_{in} is not strongly connected, and we perform an iterative edge reversal procedure. We build a condensation graph $\mathcal{D}(\mathcal{V}, \mathcal{E})$ (algorithm 1) following Cormen *et al.* [2009] by contracting each SCC into a vertex in \mathcal{V} . Since \mathcal{D} is a DAG [Cormen *et al.*, 2009], we can find a source meta vertex $\eta \in \mathcal{V}$ s.t. η has no incoming edges (algorithm 1). We then find all outgoing edges $E_{out} \subseteq E_{in}$ of the vertices in the SCC of G_{in} corresponding to η (algorithm 1) and sample half of them as E_{rev} (algorithm 1). If $|E_{out}| = 1$, there are no edges in $|E_{rev}|$. We prove that $|E_{out}| \geq 2$ and thus $|E_{rev}| \geq 1$ in Section A.1. We reverse the direction of the edges in E_{rev} while maintaining their edge weights (algorithm 1) and run the Tarjan algorithm to check for updated SCCs (algorithm 1). We return G_{in} when it has exactly 1 SCC (algorithm 1). Intuitively, reversing directions of the edges in E_{rev} allows η to have incoming edges in \mathcal{D} , potentially reducing the number of SCCs in G_{in} . Although ERS is not a complete algorithm, it runs very fast with each iteration taking $O(|E_{in}| + |V_{in}|)$. Empir-

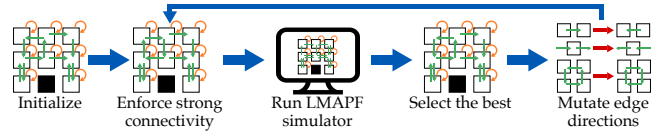


Figure 2: Optimize edge directions in phase one of MGGO-DS.

ically, ERS always returns a valid solution. We provide experimental evaluations of ERS compared to an optimal MILP solver [Duhamel and Santos, 2024] in Section A.2.

4.2 Two-Phase MGGO-DS

Phase One: Optimizing Edge Directions

In phase one, we optimize the edge directions of the mixed guidance graph by assigning a direction to *all* non-bridge edges in $G(V, E)$. We define a binary decision variable for each undirected non-bridge edge $\{u,v\} \in E$. The binary variable determines whether $\{u,v\}$ is changed to (u,v) or (v,u) . We do not include the option to make $\{u,v\}$ bidirected in the decision variable because an unweighted bidirected edge does not provide any guidance and, therefore, would be abandoned by the optimizer.

We optimize the edge directions using $(1 + \lambda)$ Evolutionary Algorithm (EA) [Back *et al.*, 1997]. Figure 2 shows the overview. After initializing a batch of λ mixed guidance graphs, we repair the graphs for strong connectivity and evaluate each of them by running LMAPF simulations N_e times for T timesteps. We select the one with the highest throughput and mutate it, generating λ new graphs. We then repair them with ERS and evaluate the mutated graphs in the simulator. We stop when the number of evaluations reaches N_{eval} .

Initialization. We use three initialization methods. (1) *directed Crisscross*: the original Crisscross alternates directions every 1 column or row. We generalize it to alternate directions every p rows and columns $\forall p \in \{1, 2, \dots, \lfloor \frac{\min(H,W)}{2} \rfloor\}$, where H and W are the height and width of the grid graph, respectively. (2) *DFS* [Roberts, 1978]: we use DFS to generate different strongly connected mixed guidance graphs. (3) *random*: we generate random directed graphs. With a batch size λ , we perform each initialization on one-third of the batch.

Mutation. Inspired by previous works [Gallo *et al.*, 2010; Fontaine *et al.*, 2019], we use three mutation operators. (1) *k-edges*: we randomly sample k distinct edges and change their directions. (2) *k-vertices*: we randomly sample k distinct vertices and change the directions of all their incoming and outgoing edges. In these two operators, k is sampled from a geometric distribution $P(X = k) = (1 - p)^{k-1}p$ with $p = \frac{1}{2}$. (3) *random-cycle*: we first select a random vertex and perform a DFS from it to find a random cycle. Since the graph before mutation is guaranteed to be strongly connected, at least one cycle exists in the graph. We then change the directions of all the edges in the cycle. With a batch size λ , we perform each mutation on one-third of the batch.

Phase Two: Optimizing Edge Weights

After optimizing the edge directions in phase one, we obtain an unweighted mixed guidance graph $G_{mg}(V, E_{mg}, \mathbf{1}^{|E_{mg}|})$.

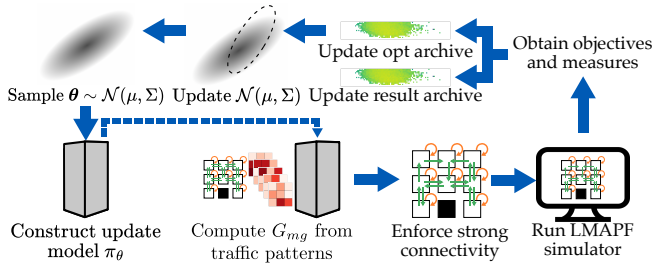


Figure 3: QD-based Joint MGGO-PU.

We then use GGO-DS [Zhang *et al.*, 2024] to optimize the edge weights, forming $G_{mg}(V, E_{mg}, \omega_{mg})$.

4.3 QD-based Joint MGGO-PU

Although the two-phase search can optimize both the edge directions and the edge weights, it maximizes the number of unidirectional edges. Agents can take unnecessary detours with too many unidirectional edges. Therefore, we present joint MGGO-PU, where edge directions and edge weights are optimized jointly. Figure 3 shows the overview. We use CMA-MAE [Fontaine and Nikolaidis, 2023] to optimize the parameters of an update model, which generates mixed guidance graphs given precomputed traffic patterns. We first sample from the multi-variate Gaussian of CMA-MAE for a batch of λ parameter vectors, forming update models. Based on precomputed traffic patterns, we use update models to generate the mixed guidance graphs. We then repair the graphs with ERS, evaluate them in the LMAPF simulator, and compute the objectives and measures. We then add the evaluated guidance graphs and the corresponding update models to an optimization archive and a result archive. Finally, we update the parameters of the Gaussian. We run CMA-MAE until the total number of evaluations reaches N_{eval} .

Precomputed Traffic Patterns

To obtain the traffic pattern, we run N_{obs} LMAPF simulations in an unweighted guidance graph and a directed Crisscross mixed guidance graph generated based on directed Crisscross highways [Li and Sun, 2023]. We run ERS on the generated directed Crisscross to ensure strong connectivity. Each simulation produces a $[H, W, 7]$ tensor that encodes the frequencies of move actions in four directions and the frequencies for waiting and clockwise/counterclockwise rotations. We feed the traffic pattern along with the initial guidance graphs to the update model to generate the resulting mixed guidance graphs. We use directed Crisscross because it is the state-of-the-art human-designed guidance graph [Zhang *et al.*, 2024], and we make it directed to give the model more information on how edge directions provide guidance.

Update Model and Graph Representation

We need to define an update model and represent the edge weights and edge directions of a mixed guidance graph for a grid graph of size $H \times W$. We follow Zhang *et al.* [2024] to represent the edge weights as a tensor of size $[H, W, 5]$, where the five channels represent the edge weights of the four outgoing edges at each vertex and the cost of waiting. We represent the edge directions differently in the input and output.

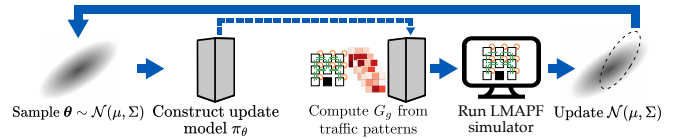


Figure 4: Edge-Direction-Aware GGO-PU.

Setup	MAPF	Map	$ E_{mg,max} $	$ X $	N_a
1		random-32-32-20	3,359	1,258	200
2	RHCR	warehouse-33-36	4,074	1,563	220
3		empty-48-48	11,328	4,512	800
4		random-32-32-20	3,359	1,258	400
5		warehouse-33-36	4,074	1,563	400
6	PIBT	empty-48-48	11,328	4,512	1,000
7		room-64-64-8	14,340	5,535	1,500
8		den312d	11,227	4,369	1,200

Table 1: Summary of the experiment setup. $|E_{mg,max}|$ is the maximum number of edges the mixed guidance graphs can have, respectively. $|X|$ is the number of decision variables in phase-one of two-phase MGGO-DS. N_a is the number of agents.

In the input, we use an *independent representation*, where the edge directions are represented as a $[H, W, 4]$ tensor. The four channels are binary variables that indicate whether an outgoing edge exists from the corresponding vertices. However, this cannot be used in the output. For a pair of vertices u and v , if the model outputs 0 for both (u, v) and (v, u) , there are no edges between u and v . Therefore, we use a *dependent representation* in the output with a tensor of size $[H, W, 6]$. The first 3 and the last 3 channels represent a one-hot encoding of the outgoing edges to the east and south, respectively. For a vertex u and its eastern neighbor v , for example, the first 3 values indicate the probability of having edge (u, v) , (v, u) , or both (u, v) and (v, u) , respectively. Since CMA-MAE is sensitive to the dimension of the search space, we use the independent representation in the input to keep the update model small and the dependent representation in the output to ensure that the model always gives a valid decision. Therefore, our update model is a CNN that takes in a tensor of size $[H, W, 2 \cdot 7 \cdot N_{obs} + 2 \cdot 9]$ and outputs a tensor of size $[H, W, 11]$.

Objectives and Diversity Measure

We have two objectives, f_{opt} and f_{res} , corresponding to the optimization archive and the result archive. f_{res} runs N_e LMAPF simulations and computes the average throughput, while $f_{opt} = f_{res} + \alpha \cdot \Delta$, computing a weighted sum of f_{res} and an edge direction similarity score Δ . Δ quantifies the ratio of edges that are reversed by ERS, and α is a hyperparameter. We use CMA-MAE to maximize f_{opt} in the optimization archive while keeping the high-throughput guidance graphs in the result archive. We incorporate Δ to f_{opt} as a regularization term to encourage the model to directly generate strongly connected mixed guidance graphs, reducing the dependency on ERS. Zhang *et al.* [2023] used a similar regularization technique to improve the results of QD optimization. We use one diversity measure, namely the ratio of

unidirectional edges, to control the trade-off between reducing head-on collisions and taking fewer detours in the graph.

4.4 Edge-Direction-Aware GGO-PU

We attempt to enhance GGO-PU by making it *edge-direction-aware*, meaning that the update model observes and understands the effectiveness of unidirectional edges in providing guidance and learns to generate guidance graphs. Figure 4 shows the overview of GGO-PU. We use CMA-ES to search for the parameters of an update model capable of generating high-throughput guidance graphs. The key to making GGO-PU edge-direction-aware is using the same traffic pattern from Section 4.3 as it includes the traffic pattern observed from a directed Crisscross guidance graph.

5 Experimental Evaluation

5.1 Experimental Setup

General Setup

Table 1 shows the experimental setups. Column 2 shows the LMAPF algorithms, namely PIBT [Jiang *et al.*, 2024] and RHCR [Li *et al.*, 2021] with $w = 5$, $h = 2$, and a runtime limit of 2 seconds for each MAPF run. During optimization, we use $N_e = 10$, $T = 2,000$ for PIBT and $N_e = 5$, $T = 1,000$ for RHCR to obtain throughput. Column 3 shows the maps, including one commonly used warehouse map [Li *et al.*, 2021] and four chosen from the MAPF benchmark [Stern *et al.*, 2019]. Column 4 shows the maximum number of edges $|E_{mg-max}|$ that the optimized mixed guidance graph can have. Column 5 shows the number of decision variables in phase one of the two-phase MGGO-DS. Column 6 shows the number of agents N_a used to optimize the mixed guidance graphs. For the QD-based Joint MGGO-PU, we use $\alpha = 3$. We run all algorithms with $N_{eval} = 20,000$. For the two-phase MGGO-DS, we assign 5,000 and 15,000 evaluations to phase one and phase two, respectively. We show the implementation details and compute resources in Section B.1.

Baselines

We compare with three baselines: (1) CMA-ES + GGO-DS [Zhang *et al.*, 2024], the state-of-the-art method for GGO, (2) Directed Crisscross [Cohen, 2020], the state-of-the-art human-designed guidance graph, and (3) No Guidance, where all edge weights are 1. We do not include GGO-PIU because it does not outperform GGO-DS [Zhang *et al.*, 2024].

Precomputed Traffic Patterns and Update Models

We use $N_{obs} = 2$ to collect traffic patterns, resulting in an input of size $[H, W, 46]$ to the update model. Our update model is a CNN with 3 convolutional layers with kernel sizes 3×3 , 1×1 , and 1×1 , respectively. All convolutional layers have 8 hidden channels and are followed by a ReLU activation and a batch norm layer, resulting in 3,479 parameters.

5.2 Experimental Result

Proposed Methods vs. Baselines

We run all optimized (mixed) guidance graphs with various numbers of agents, each for 50 simulations, and show the results in Figures 5 and 6. We show throughput and the ratio of agents that wait and rotate at each timestep (Ts). The solid

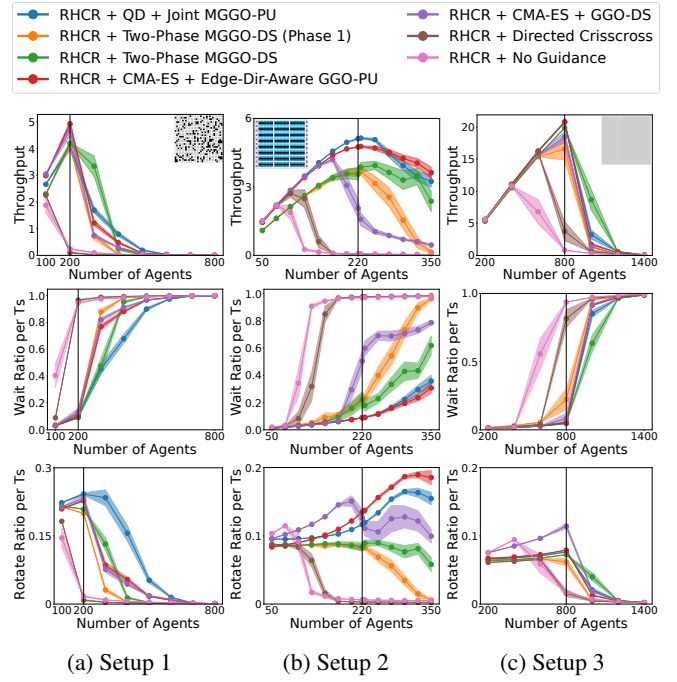


Figure 5: Throughput, wait action ratio, and rotation action ratio with different numbers of agents for RHCR in setups 1 to 3.

lines are the average, and the shaded areas are 95% confidence intervals. The black vertical lines indicate N_a .

With PIBT, one of our proposed methods always achieves the highest throughput, but the best method varies across setups. Interestingly, maximizing the number of unidirectional edges with the two-phase MGGO-DS reduces the ratio of rotation actions, potentially at the cost of more waiting. This is because unidirectional edges can prevent agents from taking suboptimal detours, especially with PIBT. This helps the two-phase MGGO-DS to achieve the highest throughput in random-32-32-20, room-64-64-8, and den312d. In empty-48-48, however, agents have more space to coordinate, so using edge-direction-aware GGO-PU to optimize the edge weights outperforms all MGGO methods. Nevertheless, our edge-direction-aware GGO-PU outperforms GGO-DS on most maps, highlighting the importance of incorporating edge-direction-related information into GGO. In warehouse-33-36, the QD-based Joint MGGO-PU achieves the best performance, while the other two proposed methods achieve similar performance, indicating the need for joint optimization.

With RHCR in setup 2, the QD-based Joint MGGO-PU achieves the highest throughput in warehouse-33-36, and unidirectional edges are helpful in terms of reducing the rotation action ratio. However, for setups 1 and 3, optimizing edge directions is less helpful, and we do not observe significant differences on the ratio of rotation actions in these setups. Equipped with an optimal low-level planner, RHCR is less inclined to have agents traversing the high-cost edges than PIBT. Therefore, optimizing edge weights is good enough in most cases for RHCR. Nevertheless, providing

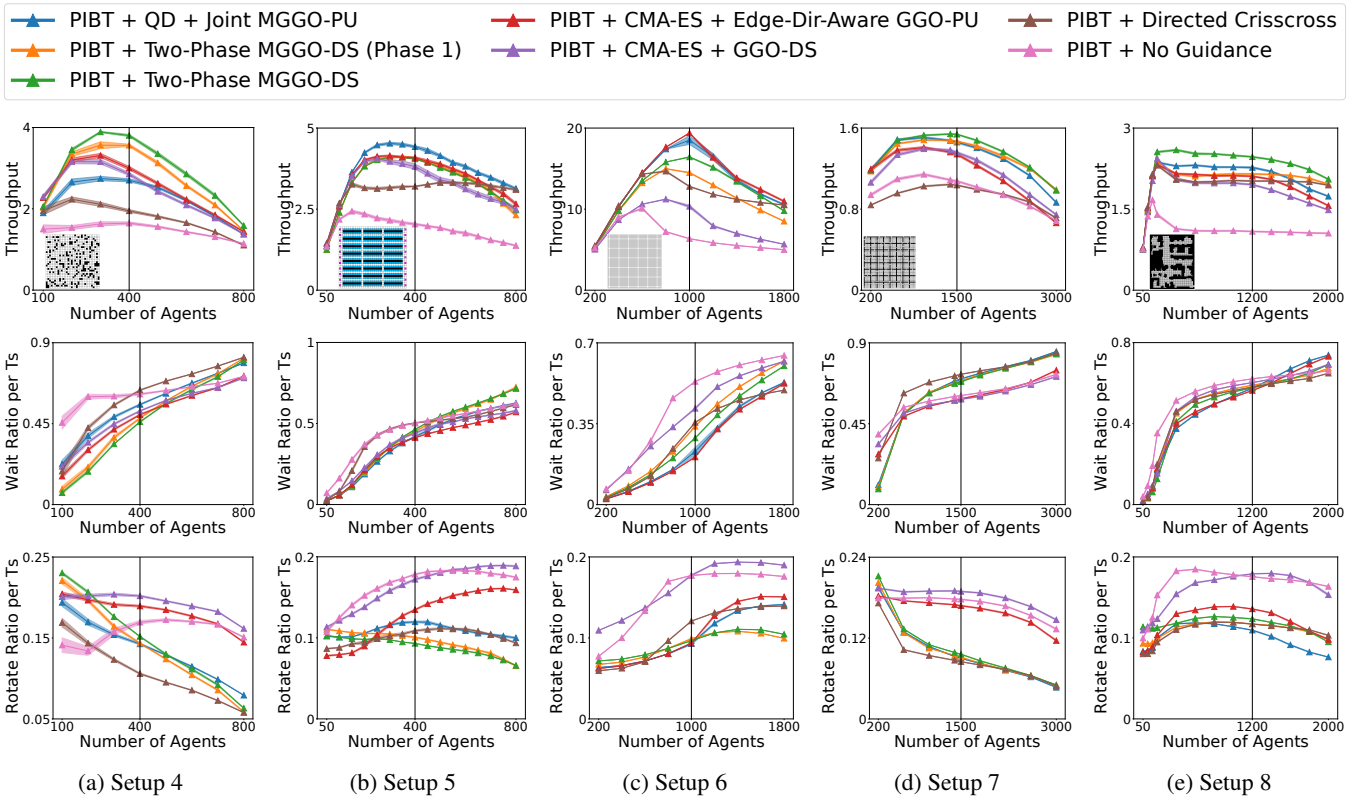


Figure 6: Throughput, wait action ratio, and rotation action ratio with different numbers of agents for PIBT in setups 4 to 8.

MGGO	Throughput	CPU Runtime
QD + Joint MGGO-PU	4.42 ± 0.02	2.76 ± 0.03
CMA-ES + Joint MGGO-PU	4.26 ± 0.01	3.35 ± 0.01
QD + Joint MGGO-PU (Indept Edge-Dir Rep)	4.18 ± 0.01	2.57 ± 0.01
MGGO-DS (Phase 1)	4.07 ± 0.01	2.40 ± 0.02
MGGO-DS (Phase 1, Bi-Dir)	3.93 ± 0.01	3.03 ± 0.02
MGGO-DS (Phase 1, k-node Only)	3.86 ± 0.01	3.01 ± 0.02
MGGO-DS (Phase 1, k-node/k-edge Only)	3.90 ± 0.01	2.76 ± 0.02

Table 2: Numerical results of ablation experiments. We run each graph for 50 times and report the results in the format of $x \pm y$, where x and y are the average and standard error, respectively.

edge-direction-related information to GGO continues to be helpful, allowing edge-direction-aware GGO-PU to achieve the best throughput in setups 1 and 3. We show additional numerical results at N_a in Section B.2.

Ablations

Variants of Joint MGGO-PU. We compare our proposed QD-based Joint MGGO-PU with two variants to justify our design choices: (1) CMA-ES + Joint MGGO-PU, where we use CMA-ES to directly optimize throughput to show the necessity of using QD and regularizing with edge similarity scores, and (2) QD + Joint MGGO-PU (Indept Edge-Dir Rep), where we use the independent edge direction representation from Section 4.3 in both input and output of the update model to justify our choice of representation. We use the same N_e , N_{eval} , and T in setup 5. We present the result with $N_a = 400$ agents in Table 2, showing that our proposed Joint

MGGO-PU method achieves the highest throughput.

Variants of $(1 + \lambda)$ EA in MGGO-DS Phase One. We compare our proposed $(1 + \lambda)$ EA with three variants: (1) MGGO-DS (Phase 1, Bi-Dir), where the decision variables can assign an edge to be bidirected, (2) MGGO-DS (Phase 1, k -vertices Only), where only the k -vertices mutation operator is used, and (3) MGGO-DS (Phase 1, k -vertices/ k -edges Only), where only k -vertices and k -edges mutation operators are used. Table 2 shows that including bidirected edges does not help optimize the edge directions. In addition, using diverse mutation operators helps with optimizations. We show more ablation results in Sections B.3 and B.4, and example optimized mixed guidance graphs in Section C.

6 Conclusion

We extend GGO to MGGO by optimizing both edge directions and weights, and introduce ERS, a fast algorithm to enforce strong connectivity via edge reversals. We also incorporate edge-direction-related information to GGO. Empirically, our proposed methods outperform the baselines, establishing a new state-of-the-art for guidance in LMAPF. We discover that edge directions are more beneficial for rule-based planners such as PIBT, primarily by reducing rotation actions while offering more limited gains for search-based methods such as RHCR. However, MGGO does not consistently outperform all GGO variants, likely because of reduced sample efficiency due to increased complexity. Future work may im-

prove sample efficiency via surrogate modeling [Zhang *et al.*, 2022].

Acknowledgments

This work is in part supported by the National Science Foundation (NSF) under grant numbers #2328671 and #2441629, as well as a gift from Amazon. This work used Bridge-2 at Pittsburgh Supercomputing Center (PSC) [Brown *et al.*, 2021] through allocation CIS220115 from the Advanced Cyberinfrastructure Coordination Ecosystem: Services & Support (ACCESS) program, which is supported by NSF under grant numbers #2138259, #2138286, #2138307, #2137603, and #2138296.

References

- [Back *et al.*, 1997] Thomas Back, David B. Fogel, and Zbigniew Michalewicz. *Handbook of Evolutionary Computation*. IOP Publishing Ltd., GBR, 1st edition, 1997.
- [Bhatt *et al.*, 2022] Varun Bhatt, Bryon Tjanaka, Matthew Fontaine, and Stefanos Nikolaidis. Deep surrogate assisted generation of environments. In *Proceedings of the Advances in Neural Information Processing Systems (NeurIPS)*, pages 37762–37777, 2022.
- [Brown *et al.*, 2021] Shawn T. Brown, Paola Buitrago, Edward Hanna, Sergiu Sanielevici, Robin Scibek, and Nicholas A. Nystrom. Bridges-2: A platform for rapidly-evolving and data intensive research. In *Proceedings of the Practice and Experience in Advanced Research Computing (PEARC): Evolution Across All Dimensions*, PEARC '21, 2021.
- [Burkard *et al.*, 1999] Rainer E. Burkard, Karin Feldbacher, Bettina Klinz, and Gerhard J. Woeginger. Minimum-cost strong network orientation problems: Classification, complexity, and algorithms. *Networks*, 33(1):57–70, January 1999.
- [Chen *et al.*, 2024] Zhe Chen, Daniel Harabor, Jiaoyang Li, and Peter Stuckey. Traffic flow optimisation for lifelong multi-agent path finding. In *Proceedings of the AAAI Conference on Artificial Intelligence (AAAI)*, pages 20674–20682, 2024.
- [Cohen *et al.*, 2015] Liron Cohen, Tansel Uras, and Sven Koenig. Feasibility study: Using highways for bounded-suboptimal multi-agent path finding. In *Proceedings of the International Symposium on Combinatorial Search (SoCS)*, pages 2–8, 2015.
- [Cohen *et al.*, 2016] Liron Cohen, Tansel Uras, T. K. Satish Kumar, Hong Xu, Nora Ayanian, and Sven Koenig. Improved solvers for bounded-suboptimal multi-agent path finding. In *Proceedings of the International Joint Conference on Artificial Intelligence (IJCAI)*, pages 3067–3074, 2016.
- [Cohen, 2020] Liron Cohen. *Efficient Bounded-Suboptimal Multi-Agent Path Finding and Motion Planning via Improvements to Focal Search*. PhD thesis, University of Southern California, 2020.
- [Cormen *et al.*, 2009] Thomas H. Cormen, Charles E. Leiserson, Ronald L. Rivest, and Clifford Stein. *Introduction to Algorithms, Third Edition*. The MIT Press, 3rd edition, 2009.
- [Duhamel and Santos, 2024] Christophe Duhamel and Andréa Cynthia Santos. The strong network orientation problem. *International Transactions in Operational Research*, 31(1):192–220, 2024.
- [Erdmann and Lozano-Perez, 1986] M. Erdmann and T. Lozano-Perez. On multiple moving objects. In *Proceedings. 1986 IEEE International Conference on Robotics and Automation*, volume 3, pages 1419–1424, 1986.
- [Fontaine and Nikolaidis, 2023] Matthew Fontaine and Stefanos Nikolaidis. Covariance matrix adaptation map-annealing. In *Proceedings of the Genetic and Evolutionary Computation Conference (GECCO)*, pages 456–465, 2023.
- [Fontaine *et al.*, 2019] Matthew C Fontaine, Scott Lee, Lisa B Soros, Fernando de Mesentier Silva, Julian Togelius, and Amy K Hoover. Mapping hearthstone deck spaces through MAP-elites with sliding boundaries. In *Proceedings of The Genetic and Evolutionary Computation Conference (GECCO)*, pages 161–169, 2019.
- [Fontaine *et al.*, 2021] Matthew C. Fontaine, Ruilin Liu, Ahmed Khalifa, Jignesh Modi, Julian Togelius, Amy K. Hoover, and Stefanos Nikolaidis. Illuminating Mario scenes in the latent space of a generative adversarial network. *Proceedings of the AAAI Conference on Artificial Intelligence (AAAI)*, pages 5922–5930, 2021.
- [Gallo *et al.*, 2010] Mariano Gallo, Luca D’Acierno, and Bruno Montella. A meta-heuristic approach for solving the Urban Network Design Problem. *European Journal of Operational Research*, 201(1):144–157, 2010.
- [Gaskins and Tanchoco, 1987] R. J. Gaskins and J. M. A. Tanchoco. Flow path design for automated guided vehicle systems. *International Journal of Production Research*, 25(5):667–676, May 1987.
- [Han and Yu, 2022] Shuai D. Han and Jingjin Yu. Optimizing space utilization for more effective multi-robot path planning. In *Proceedings of the International Conference on Robotics and Automation (ICRA)*, pages 10709–10715, 2022.
- [Hansen, 2016] Nikolaus Hansen. The CMA evolution strategy: A tutorial. *ArXiv*, abs/1604.00772, 2016.
- [Jansen and Sturtevant, 2008] M. Renee Jansen and Nathan R Sturtevant. Direction maps for cooperative pathfinding. In *Proceedings of the AAAI Conference on Artificial Intelligence and Interactive Digital Entertainment (AIIDE)*, pages 185–190, 2008.
- [Jiang *et al.*, 2024] He Jiang, Yulun Zhang, Rishi Veerapaneni, and Jiaoyang Li. Scaling lifelong multi-agent path finding to more realistic settings: Research challenges and opportunities. In *Proceedings of the International Symposium on Combinatorial Search (SoCS)*, pages 234–242, 2024.

- [Kaspi and Tanchoco, 1990] Moshe Kaspi and J. M. A. Tanchoco. Optimal flow path design of unidirectional AGV systems. *International Journal of Production Research*, 28(6):1023–1030, June 1990.
- [Kou *et al.*, 2020] Ngai Meng Kou, Cheng Peng, Hang Ma, T. K. Satish Kumar, and Sven Koenig. Idle time optimization for target assignment and path finding in sortation centers. In *Proceedings of the AAAI Conference on Artificial Intelligence (AAAI)*, pages 9925–9932, 2020.
- [Li and Sun, 2023] Ming-Feng Li and Min Sun. The study of highway for lifelong multi-agent path finding. *ArXiv*, 2304.04217, 2023.
- [Li *et al.*, 2021] Jiaoyang Li, Andrew Tinka, Scott Kiesel, Joseph W. Durham, T. K. Satish Kumar, and Sven Koenig. Lifelong multi-agent path finding in large-scale warehouses. In *Proceedings of the AAAI Conference on Artificial Intelligence (AAAI)*, pages 11272–11281, 2021.
- [Ma *et al.*, 2017] Hang Ma, Jingxing Yang, Liron Cohen, T. K. Satish Kumar, and Sven Koenig. Feasibility study: Moving non-homogeneous teams in congested video game environments. In *Proceedings of the AAAI Conference on Artificial Intelligence and Interactive Digital Entertainment (AIIDE)*, pages 270–272, 2017.
- [Ma *et al.*, 2019] Hang Ma, Daniel Harabor, Peter J. Stuckey, Jiaoyang Li, and Sven Koenig. Searching with consistent prioritization for multi-agent path finding. In *Proceedings of the AAAI Conference on Artificial Intelligence (AAAI)*, pages 7643–7650, 2019.
- [Okumura *et al.*, 2019] Keisuke Okumura, Manao Machida, Xavier Défago, and Yasumasa Tamura. Priority inheritance with backtracking for iterative multi-agent path finding. In *Proceedings of the International Joint Conference on Artificial Intelligence (IJCAI)*, pages 535–542, 2019.
- [Paszke *et al.*, 2019] Adam Paszke, Sam Gross, Francisco Massa, Adam Lerer, James Bradbury, Gregory Chanan, Trevor Killeen, Zeming Lin, Natalia Gimelshein, Luca Antiga, Alban Desmaison, Andreas Kopf, Edward Yang, Zachary DeVito, Martin Raison, Alykhan Tejani, Sasank Chilamkurthy, Benoit Steiner, Lu Fang, Junjie Bai, and Soumith Chintala. PyTorch: An imperative style, high-performance deep learning library. In *Proceedings of the Advances in Neural Information Processing Systems (NeurIPS)*, pages 8024–8035, 2019.
- [Phillips and Likhachev, 2011] Mike Phillips and Maxim Likhachev. SIPP: Safe interval path planning for dynamic environments. In *Proceedings of the IEEE International Conference on Robotics and Automation (ICRA)*, pages 5628–5635, 2011.
- [Qian *et al.*, 2024] Chao Qian, Ke Xue, and Ren-Jian Wang. Quality-diversity algorithms can provably be helpful for optimization. In *Proceedings of the International Joint Conference on Artificial Intelligence (IJCAI)*, pages 6994–7002, 2024.
- [Robbins, 1939] H. E. Robbins. A Theorem on Graphs, with an Application to a Problem of Traffic Control. *The American Mathematical Monthly*, 46(5):281, May 1939.
- [Roberts, 1978] Fred S. Roberts. *Graph Theory and Its Applications to Problems of Society*, volume 29 of *CBMS-NSF Regional Conference Series in Applied Mathematics*. Society for Industrial and Applied Mathematics (SIAM), 1978.
- [Silver, 2005] David Silver. Cooperative pathfinding. In *Proceedings of the Artificial Intelligence and Interactive Digital Entertainment Conference (AIIDE)*, pages 117–122, 2005.
- [Stern *et al.*, 2019] Roni Stern, Nathan R. Sturtevant, Ariel Felner, Sven Koenig, Hang Ma, Thayne T. Walker, Jiaoyang Li, Dor Atzmon, Liron Cohen, T. K. Satish Kumar, Roman Barták, and Eli Boyarski. Multi-agent pathfinding: Definitions, variants, and benchmarks. In *Proceedings of the International Symposium on Combinatorial Search (SoCS)*, pages 151–159, 2019.
- [Tarjan, 1972] Robert Tarjan. Depth-first search and linear graph algorithms. *SIAM Journal on Computing*, 1(2):146–160, 1972.
- [Tarjan, 1974] R. Endre Tarjan. A note on finding the bridges of a graph. *Information Processing Letters*, 2(6):160–161, April 1974.
- [Tjanaka *et al.*, 2023] Bryon Tjanaka, Matthew C. Fontaine, David H. Lee, Yulun Zhang, Nivedit Reddy Balam, Nathaniel Dennler, Sujay S. Garlanka, Nikitas Dimitri Klapsis, and Stefanos Nikolaidis. pyribs: A bare-bones python library for quality diversity optimization. In *Proceedings of the Genetic and Evolutionary Computation Conference (GECCO)*, pages 220–229, 2023.
- [Wang and Botea, 2008] Ko-Hsin Cindy Wang and Adi Botea. Fast and memory-efficient multi-agent pathfinding. In *Proceedings of the International Conference on Automated Planning and Scheduling (ICAPS)*, pages 380–387, 2008.
- [Yan and Li, 2025] Jingtian Yan and Jiaoyang Li. Multi-agent motion planning for differential drive robots through stationary state search. In *AAAI Conference on Artificial Intelligence*, pages 23360–23368, 2025.
- [Yu and Wolf, 2023] Ge Yu and Michael Wolf. Congestion prediction for large fleets of mobile robots. In *Proceedings of the International Conference on Robotics and Automation (ICRA)*, pages 7642–7649, 2023.
- [Yukhnevich and Andreychuk, 2025] Egor Yukhnevich and Anton Andreychuk. Enhancing PIBT via multi-action operations. In *Proceedings of the AAAI Conference on Artificial Intelligence (AAAI)*, 2025.
- [Zhang *et al.*, 2022] Yulun Zhang, Matthew C. Fontaine, Amy K. Hoover, and Stefanos Nikolaidis. Deep surrogate assisted map-elites for automated hearthstone deckbuilding. In *Proceedings of the Genetic and Evolutionary Computation Conference (GECCO)*, pages 158–167, 2022.
- [Zhang *et al.*, 2023] Yulun Zhang, Matthew C. Fontaine, Varun Bhatt, Stefanos Nikolaidis, and Jiaoyang Li. Arbitrarily scalable environment generators via neural cellular automata. In *Proceedings of the Advances in Neural*

Information Processing Systems (NeurIPS), pages 57212–57225, 2023.

[Zhang *et al.*, 2024] Yulun Zhang, He Jiang, Varun Bhatt, Stefanos Nikolaidis, and Jiaoyang Li. Guidance graph optimization for lifelong multi-agent path finding. In *Proceedings of the International Joint Conference on Artificial Intelligence (IJCAI)*, pages 311–320, 2024.

[Zhang *et al.*, 2025] Yulun Zhang, Alexandre O. G. Barbosa, Federico Pecora, and Jiaoyang Li. Destination-to-chutes task mapping optimization for multi-robot coordination in robotic sorting systems. In *Proceedings of the IEEE International Symposium on Multi-Robot and Multi-Agent Systems (MRS)*, 2025.

A Theoretical and Empirical Results of ERS

A.1 Proof

Lemma 1. *The condensation graph \mathcal{D} is weakly connected.*

Proof. According to Cormen *et al.* [2009], \mathcal{D} is a DAG. Therefore, \mathcal{D} is trivially weakly connected. \square

Theorem 1. *If, from a meta vertex $\eta \in \mathcal{V}$ s.t. $\deg^-(\eta) = 0$, we follow ERS to find the set of edges E_{rev} , then $|E_{rev}| \geq 1$.*

Proof. For the sake of contradiction, assume that $|E_{rev}| = 0$. Then $|E_{out}| \leq 1$.

If $|E_{out}| = 0$, there are no edges between η and other meta vertices, contradicting Lemma 1.

If $|E_{out}| = 1$, there is only 1 vertex $v \in V_{in}$ in the SCC that corresponds to η in G_{in} . Let the SCC be C_η . Then the edge $e = (v, u) \in E_{in}$ that goes from v to a vertex $u \notin C_\eta$ must be a bridge. This is because removing e will disconnect v from G_{in} . Since all bridges are assumed to be bidirected in G_{in} , which means that they cannot be directed edges between different SCCs, this contradicts the fact that e is a bridge. Therefore, $|E_{out}| \geq 2$, and thus $|E_{rev}| \geq 1$. \square

A.2 Empirical Evaluation

Experiment Setup

We compare ERS with a MILP solver that reverses edges to ensure strong connectivity of a graph while optimizing the number of reversed edges. We formulate the MILP based on a prior work [Duhamel and Santos, 2024]. To compare the MILP and our ERS, we generate directed four-connected empty grid graphs of different sizes and run both algorithms to repair them for strong connectivity. For each graph, we generate 10 instances and give a 1 minute time limit to both methods. We measure (1) the number of reversed edges, (2) the CPU runtime, and (3) the success rate, defined as the number of graphs that each algorithm successfully solved without timeout.

Experiment Result

Figure 7 shows the result. Although ERS has a much worse solution quality compared to MILP (that is, ERS reverses more edges than MILP), it has a runtime significantly faster than MILP. This is especially important for an evolutionary-based solver such as CMA-ES for CMA-MAE because we run these methods for each generated mixed guidance graph. Using ERS can make the optimization process much faster. In addition, with a 1 minute time limit, the success rate of MILP drops to about 60% in graphs with more than 3,000 vertices, while ERS maintains a success rate of 100%.

B Additional Experiments

B.1 Implementation and Compute Resources

Implementation

We implement CMA-ES and CMA-MAE in Python with Pyribs [Tjanaka *et al.*, 2023], the update model in Pytorch [Paszke *et al.*, 2019], and ERS in Python. We implement PIBT and RHCR in C++ based on prior implementations [Li *et al.*, 2021; Jiang *et al.*, 2024]. For RHCR, we use

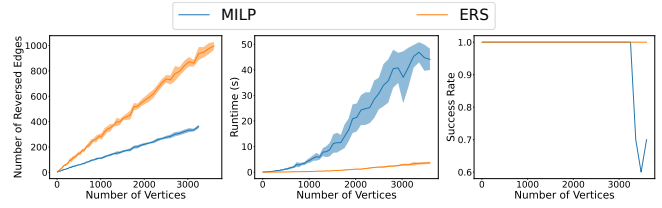


Figure 7: ERS vs. MILP.

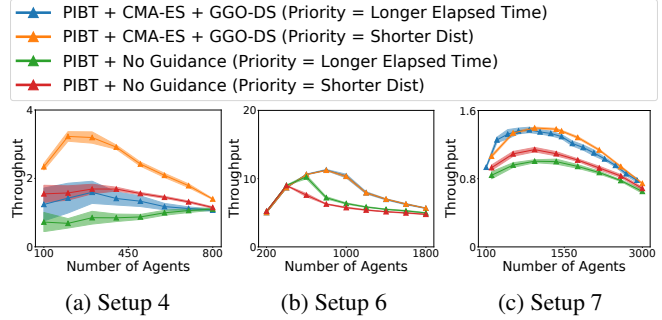


Figure 8: Comparison of different agent priority strategies of PIBT before and after GGO.

PBS [Ma *et al.*, 2019] as the MAPF solver and SIPP [Phillips and Likhachev, 2011] as the single-agent solver. To speed up optimization, we follow Zhang *et al.* [2024] to stop RHCR when the agents get congested (i.e. more than half of the agents wait in place).

Agents Priorities in PIBT We report an interesting side discovery regarding PIBT with the rotational motion model. In PIBT, agents move in a priority order. With the pebble motion model, Okumura *et al.* [2019] establishes that priorities are determined based on the number of timesteps elapsed from the point when the agents reached their last goal. Agents that arrive at their last goal earlier shall move first. On the other hand, Jiang *et al.* [2024] suggests that with the rotational motion model, it is better if the priorities are determined by the distance of the agents to their next goal. Agents closer to their next goal shall move first. We discover that, in non-biconnected maps, using the latter can significantly reduce the occurrence of deadlocks and livelocks, improving average throughput and reducing the variance in evaluation. We compare the two priority strategies before and after running GGO-DS [Zhang *et al.*, 2024] in setups 4, 6, and 7, two of which are non-biconnected (random-32-32-20 and room-64-64-8) and one of which is biconnected (empty-48-48). We present the results in Figure 8. It is clear that ordering agents by shorter distances to goals demonstrates much better performance in non-biconnected maps (setups 4 and 7). With the empty-48-48 map in setup 6, ordering with longer elapsed time demonstrates better performance, but no significant gap is discovered after GGO.

Compute Resources

We run our experiments on five machines: (1) a local machine with a 64-core AMD Ryzen Threadripper 3990X CPU, 192

Setup	MAPF + (M)GGO	SR	Throughput	CPU Runtime
1	CMA-ES + Edge-Dir-Aware GGO-PU	94%	4.93 ± 0.03	29.47 ± 0.81
	CMA-ES + GGO-DS	92%	4.69 ± 0.04	33.77 ± 0.85
	Directed Crisscross	0%	N/A	N/A
	No Guidance	0%	N/A	N/A
	QD + Joint MGGO-PU	92%	4.08 ± 0.03	32.59 ± 0.94
	Two-Phase MGGO-DS	100%	4.20 ± 0.00	18.63 ± 0.08
	Two-Phase MGGO-DS (Phase 1)	100%	4.08 ± 0.01	23.78 ± 0.16
2	CMA-ES + Edge-Dir-Aware GGO-PU	100%	4.75 ± 0.01	40.00 ± 0.20
	CMA-ES + GGO-DS	26%	2.07 ± 0.03	56.98 ± 1.33
	Directed Crisscross	0%	N/A	N/A
	No Guidance	0%	N/A	N/A
	QD + Joint MGGO-PU	100%	5.11 ± 0.01	29.70 ± 0.19
	Two-Phase MGGO-DS	82%	3.58 ± 0.01	32.41 ± 0.21
	Two-Phase MGGO-DS (Phase 1)	90%	3.64 ± 0.01	41.43 ± 0.24
3	CMA-ES + Edge-Dir-Aware GGO-PU	100%	20.81 ± 0.01	203.48 ± 0.78
	CMA-ES + GGO-DS	96%	18.44 ± 0.02	312.43 ± 1.66
	Directed Crisscross	4%	3.77 ± 0.08	226.38 ± 0.07
	No Guidance	0%	N/A	N/A
	QD + Joint MGGO-PU	100%	20.73 ± 0.01	189.15 ± 0.50
	Two-Phase MGGO-DS	100%	19.84 ± 0.01	181.16 ± 0.53
	Two-Phase MGGO-DS (Phase 1)	80%	16.56 ± 0.02	248.92 ± 1.39
4	CMA-ES + Edge-Dir-Aware GGO-PU	100%	3.00 ± 0.02	2.31 ± 0.01
	CMA-ES + GGO-DS	100%	2.85 ± 0.02	2.25 ± 0.01
	Directed Crisscross	100%	1.95 ± 0.02	2.14 ± 0.01
	No Guidance	100%	1.65 ± 0.02	2.19 ± 0.01
	QD + Joint MGGO-PU	100%	2.70 ± 0.02	2.13 ± 0.01
	Two-Phase MGGO-DS	100%	3.80 ± 0.01	2.13 ± 0.01
	Two-Phase MGGO-DS (Phase 1)	100%	3.56 ± 0.01	2.14 ± 0.01
5	CMA-ES + Edge-Dir-Aware GGO-PU	100%	4.08 ± 0.01	2.84 ± 0.02
	CMA-ES + GGO-DS	100%	3.81 ± 0.04	2.48 ± 0.02
	Directed Crisscross	100%	3.20 ± 0.01	2.42 ± 0.01
	No Guidance	100%	2.04 ± 0.01	2.42 ± 0.02
	QD + Joint MGGO-PU	100%	4.42 ± 0.02	2.76 ± 0.03
	Two-Phase MGGO-DS	100%	4.04 ± 0.00	2.56 ± 0.01
	Two-Phase MGGO-DS (Phase 1)	100%	4.07 ± 0.01	2.40 ± 0.02
6	CMA-ES + Edge-Dir-Aware GGO-PU	100%	19.39 ± 0.01	14.10 ± 0.03
	CMA-ES + GGO-DS	100%	10.34 ± 0.08	12.57 ± 0.03
	Directed Crisscross	100%	12.79 ± 0.03	12.76 ± 0.03
	No Guidance	100%	6.35 ± 0.02	11.84 ± 0.03
	QD + Joint MGGO-PU	100%	18.51 ± 0.26	14.12 ± 0.03
	Two-Phase MGGO-DS	100%	16.43 ± 0.02	12.99 ± 0.04
	Two-Phase MGGO-DS (Phase 1)	100%	14.49 ± 0.02	13.02 ± 0.03
7	CMA-ES + Edge-Dir-Aware GGO-PU	100%	1.34 ± 0.01	26.53 ± 0.06
	CMA-ES + GGO-DS	100%	1.36 ± 0.00	25.21 ± 0.06
	Directed Crisscross	100%	1.04 ± 0.00	22.42 ± 0.05
	No Guidance	100%	1.08 ± 0.00	24.81 ± 0.06
	QD + Joint MGGO-PU	100%	1.46 ± 0.00	23.01 ± 0.04
	Two-Phase MGGO-DS	100%	1.54 ± 0.00	22.73 ± 0.05
	Two-Phase MGGO-DS (Phase 1)	100%	1.47 ± 0.00	22.51 ± 0.04
8	CMA-ES + Edge-Dir-Aware GGO-PU	100%	2.11 ± 0.01	15.45 ± 0.02
	CMA-ES + GGO-DS	100%	1.95 ± 0.01	14.23 ± 0.03
	Directed Crisscross	100%	2.02 ± 0.00	14.24 ± 0.02
	No Guidance	100%	1.09 ± 0.00	13.88 ± 0.03
	QD + Joint MGGO-PU	100%	2.27 ± 0.01	15.16 ± 0.02
	Two-Phase MGGO (Phase 1 Only)	100%	2.15 ± 0.01	14.18 ± 0.02
	Two-Phase MGGO-DS	100%	2.47 ± 0.01	14.35 ± 0.03

Table 3: Success rates (SR), throughput, and CPU runtimes of the simulations on different mixed guidance graphs. For RHCR, the success rate is the percentage of simulations that end without congestion. For PIBT, it is the percentage of simulations that end without timeout. We measure the throughput and CPU runtime over only successful simulations.

GB of RAM, (2) a local machine with a 64-core AMD Ryzen Threadripper 3990X CPU, 128 GB of RAM, (3) a local machine with a 64-core AMD Ryzen Threadripper 7980X CPU, 256 GB of RAM, (4) a local machine with a 16-core AMD Ryzen 9950X CPU, 64 GB of RAM, and (5) an HPC with numerous 64-core AMD EPYC 7742 CPUs, each with 256 GB of RAM [Brown *et al.*, 2021]. We measure all CPU runtime on machine (4).

B.2 Additional Numerical Results

Table 3 shows the numerical results. We run RHCR and PIBT on all graphs with the same N_a and T in Table 1 for 50 times

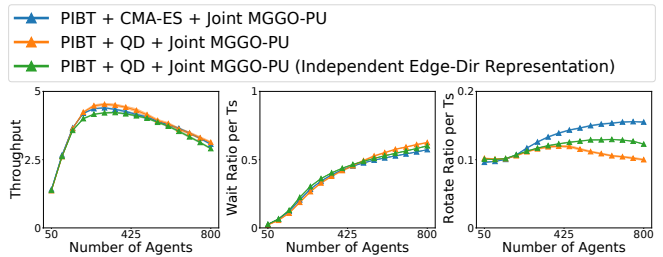


Figure 9: Throughput, wait action ratio, and rotation action ratio of Joint MGGO-PU ablations experiments.

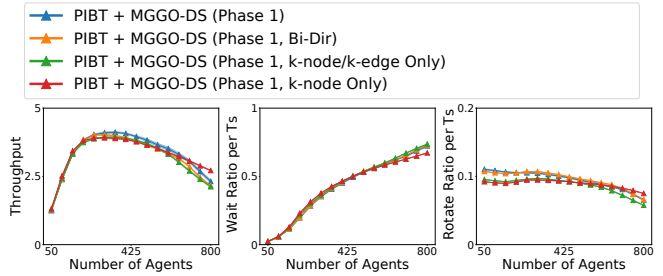


Figure 10: Throughput, wait action ratio, and rotation action ratio of $(1 + \lambda)$ EA ablations experiments.

and report the numerical results in the format of $x \pm y$, where x and y are the average and standard error, respectively. The numerical results follow the same trend with those in Figures 5 and 6.

B.3 Variant of Joint MGGO-PU

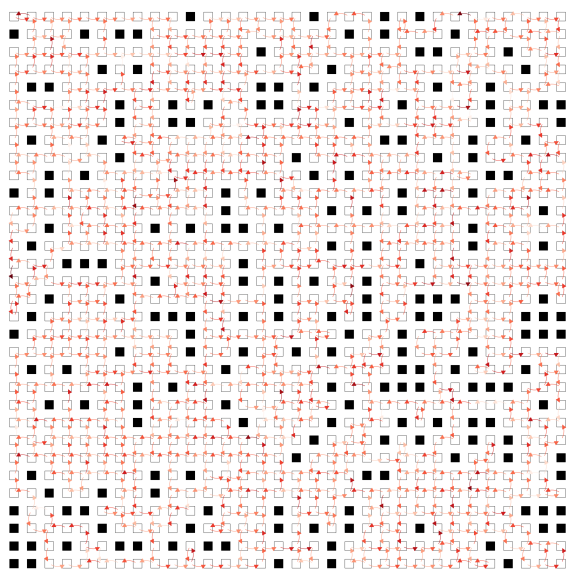
We run PIBT with different numbers of agents, each 50 times, and report the average as well as the 95% confidence interval in Figure 9. Interestingly, QD is able to reduce the ratio of rotation actions during the simulation. This is because the mixed guidance graph found by QD has about 70% of directed edges, while the one optimized by CMA-ES only has 14%.

B.4 Variants of EA in MGGO-DS Phase One

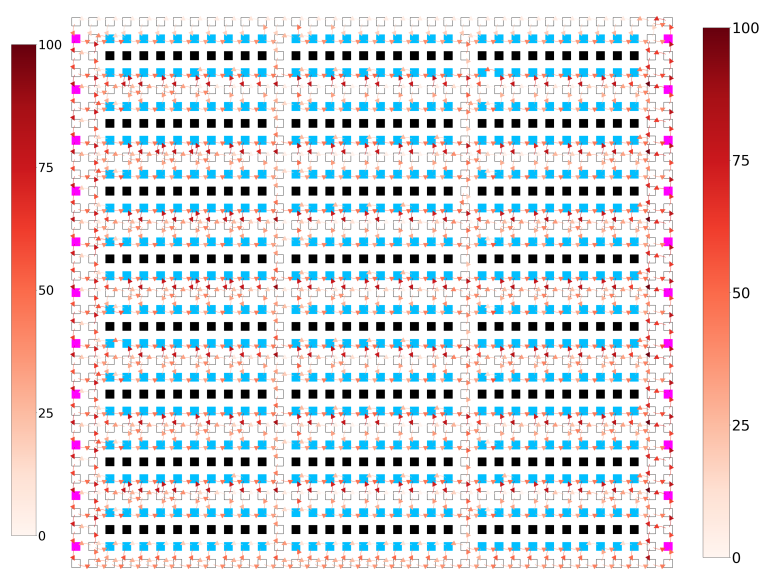
We run PIBT with different numbers of agents, each 50 times, and report the average as well as the 95% confidence interval in Figure 10. The comparison in throughput aligns with our findings in Section 5. For the ratio of waiting and rotating actions, we do not observe significant differences, as all optimized mixed guidance graphs have edge weights 1 and the number of directed edges are maximized.

C Optimized Mixed Guidance Graphs

Figure 11 shows example optimized mixed guidance graphs. Due to the size of the maps, we are only able to show the two smallest maps used in the experiments.



(a) Setup 4: random-32-32-20



(b) Setup 5: warehouse-33-36

Figure 11: Example optimized mixed guidance graphs. The arrows indicate edge directions and the color indicates edge weights.